

Modelling of processes responsible for nonlinear absorption of UV laser radiation in ionic crystals

V S Kurbasov, P B Sergeev

Abstract. Two models of interaction of UV and VUV laser radiation with MgF_2 , CaF_2 , and BaF_2 crystals are considered. In the first version, the laser radiation wavelength falls into the absorption region of F centres, in the second version it is located in the short-wavelength region of the H centre absorption wing. The photodissociation of F_2^- complexes in crystals into two holes is shown to be an efficient mechanism of defect formation in the crystal structure. The consideration of these and other processes of relaxation of electronic excitation allows one to explain many experimental effects produced by ionising and laser radiation in ionic crystals.

1. Introduction

MgF_2 and CaF_2 crystals are transparent to photons with energy up to 11 and 10 eV, respectively. They are extensively used for the fabrication of a variety of optical elements of excimer and other UV lasers, and the MgF_2 crystal virtually remains the only fairly reliable material for the fabrication of output laser windows for the VUV region. However, the transmission of these crystals, as that of other optical materials, decreases in the course of work with high-intensity short-wavelength laser radiation [1–5]. This decrease is caused mainly by the formation of colour centres during relaxation of electronic excitations produced through nonlinear absorption of intense laser radiation [4–8].

In high-power electron-beam-excited lasers, as in free-electron lasers, the material of windows is simultaneously exposed to x-rays or fast electrons in addition to laser radiation [9, 10]. However, the factors having detrimental effect upon laser windows may be useful for various technological problems related to optical-material processing, and therefore the theoretical description of the interaction of high-intensity short-wavelength laser radiation with wide-gap crystals is a topical problem.

It is known that the exposure of crystals to any ionising radiation acting on them only via the electronic subsystem leads to almost the same induced absorption, which is observed both at the moment of irradiation and after it. This absorption takes place at crystal lattice defects formed during relaxation of electronic excitations.

In the case of fluorides of rare-earth elements, ionisation occurs mainly in the anion sublattice and is accompanied by the formation of a free electron and a hole (a fluorine atom). The potential energy of this electron-hole pair relaxes in the system of levels of excitons and two pairs of anion Frenkel defects, namely, an interstitial fluorine ion (I centre) and an anionic vacancy (α centre) and also an interstitial fluorine atom (V_k and H centres) and an electron localised on an anionic vacancy (F centre). Each of these colour centres has its own absorption spectrum and, in addition to the ground state, a series of intermediate electronic states characterised by certain lifetimes [6–8, 11, 12].

It is obvious that the analysis of induced absorption in these crystals in different regimes of their exposure to ionising and laser radiation should be carried out taking into account many interrelated processes, which requires the use of numerical methods.

The aim of this paper is to reveal on the basis of numerical simulation the main features of relaxation of electronic excitations in crystals of fluorides of rare-earth elements taking into account the effect of UV laser radiation on relaxation processes. Here, we consider models of the kinetics of relaxation of electronic excitations when the laser radiation wavelength falls into the absorption band of F or H centres in MgF_2 , CaF_2 , and BaF_2 crystals.

2. Absorption of laser radiation by F centres

The irradiation of MgF_2 , CaF_2 , and BaF_2 crystals with an electron beam produces there strong absorption bands at 275, 400, and 600 nm, respectively, with the half-width of ~ 100 nm. This absorption is attributed to F centres [6, 11, 12]. However, the two-level approximation is insufficient for its description. The point is that the absorption bands are characterised by a large set of relaxation times from $\sim 10^{-9}$ to ~ 1 s!

This is explained by the fact that an important stage of the electron-hole pair relaxation during the formation of Frenkel defects is the formation of self-trapped excitons (STEs) upon the electron capture by V_k centres. They may be found in two ground states, namely, the singlet state S_1 and the triplet state S_3 . The cross sections for absorption in the S_1 and S_3 states (σ_5 and σ_6) virtually coincide with the absorption cross section of stable F centres (σ_9). This is caused by the fact that STEs can be represented as a pair of F and V_k centres spaced by a minimum distance, each of them having its own structure of the absorption spectrum, which is close to the structure of the spectrum of long-lived defects.

V S Kurbasov, P B Sergeev P N Lebedev Physics Institute, Russian Academy of Sciences, Leninskii prosp. 53, 117924 Moscow, Russia

Received 10 November 1999, revision received 14 February 2000

Kvantovaya Elektronika 30 (8) 703–709 (2000)

Translated by A N Kirkin; edited by M N Sapozhnikov

The absorption of an energy quantum transfers F centres and the electron component of excitons to one of the possible excited states (F^* and S^*) lying near the ionisation threshold. These highly excited objects are large in size and have a high probability to capture into their interaction sphere a pair centre and relax with it to the ground lattice state. The absorption of a quantum is accompanied by shaking the nearest environment of a defect, which also favours an increase in its relaxation rate [13]. This is confirmed by numerous facts of bleaching an active medium of F centres lasers. In the model presented below, this effect is taken into account by choosing a higher relaxation rate K_{78} in comparison with the rate K_{79} .

The experimental facts presented above and their modern interpretation [6–8, 11–13] determined the choice of 11 electronic states that should be taken into account in the analysis of the action of ionising and laser radiation on crystals. In the gas-kinetic approximation, one may treat these states as particles and describe their interaction with one another and laser radiation by a system of linear differential equations for the balance of concentrations of the corresponding components [14]. The use of this approach for revealing the basic features of relaxation of electronic excitations in a crystal in the presence of laser radiation in the first approximation is quite justified.

When laser radiation falls into the absorption band of F centres, the system of kinetic equations for concentrations [14] was found to be best acceptable among many other equations tried by us. It includes large information on the key processes of formation and transformation of electronic excitations in the anion sublattice of halide crystals [6–8, 11–13] and has the form

1.
$$\frac{dn}{dt} = W_1 + (K_{811}F^* + K_{911}F)I + (\sigma_4S^* + \sigma_8F^*)J - (K_{13}V_k + K_{17}H + K_{110}\alpha)n,$$
2.
$$\frac{dp}{dt} = W_1 + \sigma_{10}\alpha J - \frac{p}{\tau_2},$$
3.
$$\frac{dV_k}{dt} = \frac{p}{\tau_2} + \sigma_4S^*J - \left(\frac{1}{\tau_3} + K_{13}n\right)V_k,$$
4.
$$\frac{dS^*}{dt} = \beta J^2 + K_{13}nV_k + (\sigma_5S_1 + \sigma_6S_3)J - \left(\frac{1}{\tau_4} + K_4n + \sigma_4J\right)S^*,$$
5.
$$\frac{dS_1}{dt} = X_{45}\left(\frac{1}{\tau_4} + K_4n\right)S^* - \left(\frac{1}{\tau_5} + \frac{1}{\tau_{57}} + K_5n + \sigma_5J\right)S_1 - K_{56}n(S_1 - S_3),$$
6.
$$\frac{dS_3}{dt} = X_{46}\left(\frac{1}{\tau_4} + K_4n\right)S^* - \left(\frac{1}{\tau_6} + \frac{1}{\tau_{67}} + K_6n + \sigma_6J\right)S_3 - K_{65}n(S_3 - S_1),$$
7.
$$\frac{dH}{dt} = \frac{V_k}{\tau_3} + \frac{X_{47}S^*}{\tau_4} + \frac{S_1}{\tau_{57}} + \frac{S_3}{\tau_{67}} - (K_{17}n + K_{78}F^* + K_{79}F)H,$$

8.
$$\frac{dF^*}{dt} = K_{110}\alpha n + \sigma_9FJ - \left(\frac{1}{\tau_8} + K_8n + K_{78}H + K_{811}I + \sigma_8J\right)F^*,$$

9.
$$\frac{dF}{dt} = \frac{X_{47}S^*}{\tau_4} + \frac{S_1}{\tau_{57}} + \frac{S_3}{\tau_{67}} + \left(\frac{1}{\tau_8} + K_8n\right)F^* + \sigma_{10}\alpha J - (K_{79}H + K_{911}I + \sigma_9J)F,$$

10.
$$\frac{d\alpha}{dt} = \frac{V_k}{\tau_3} + \sigma_8F^*J - (K_{110}n + K_{1011}I + \sigma_{10}J)\alpha,$$

11.
$$\frac{dI}{dt} = K_{17}nH - (K_{811}F^* + K_{911}F + K_{1011}\alpha)I,$$

where n and p are the free-electron and hole concentrations; W_1 is the rate of ionisation produced by an external ioniser; σ_i is the absorption cross section for the i th component at the laser radiation wavelength; J is the laser radiation intensity in photon $\text{cm}^{-2} \text{s}^{-1}$; K_{ij} are the rate constants of reactions between the components i and j (the number of a component coincides with the number of its kinetic equation in the above system of equations); τ_i are relaxation times; τ_{ij} are relaxation times of the i th component in the j th one; X_{ij} are yield factors of the corresponding reactions; βJ^2 is the rate of state formation through two-photon absorption; and β is the two-photon absorption coefficient. The conditions of conservation of charge and number of atoms in a lattice give two additional relations

$$n + F^* + F = p + V_k + H, \quad H + I = F^* + F + \alpha.$$

At first glance, the system of equations presented above is cumbersome and contains many parameters. However, almost all these parameters have been found during a hundred years of study of ionic crystals or can be estimated on the basis of experimental results.

The constants K_{13} and K_{110} determine the rate of free-electron trapping to higher levels of V_k and α centres. The constant K_{17} describes a more complicated multistage process of electron capture by the H centre, which transforms into the I centre, and because of this it is somewhat smaller than the first two constants. In our calculations, we used for these parameters the values obtained in the experiments on the measurement of free-electron lifetime [6–8, 11, 12], which are obviously understated. However, our calculations showed that an increase in these values had almost no effect on the final results.

A similar situation is observed for the hole self-trapping time τ_2 . Absorption is insensitive to its decrease starting with $\tau_2 = 10^{-10}$ s. The experimental value of τ_2 is $\sim 10^{-11}$ s [6, 7]. The rate of spontaneous transformation of V_k centres into a pair of long-lived H and α centres ($1/\tau_3$) is the first parameter that was completely chosen in the course of debugging the model starting from the experimental fact that the yield factor of long-lived F^- centres during the relaxation of electron-hole pairs in MgF_2 does not exceed 5% [6]. The values of τ_4 and K_4 and of τ_2 and K_{13} for $n \sim 10^{17} \text{ cm}^{-3}$ were chosen taking into account the fact that the S_1 and S_2 states are formed in a time not greater than 10^{-10} s [6–8, 11, 12].

The lifetimes of singlet (τ_5) and triplet (τ_6) states of excitons in MgF_2 , as in many other crystals, are known with a rather high accuracy [6, 7]. The constants for quenching these states by electrons (K_5 and K_6) were estimated from the assumption that the cross section for this process was $\sim 10^{-15} \text{ cm}^2$. The rates of yield of long-lived H and F centres, which are determined by the times τ_{57} and τ_{67} , were chosen in the course of debugging the model. The mixing of these states by electrons was introduced by analogy with similar processes in excimer lasers, using correction for different collision cross sections.

The rates of interaction of 'heavy' particles (K_{78} , K_{79} , K_{811} , K_{911} , K_{1011}) are relatively low because of low linear velocities of their motion in a crystal. However, even the highest rates of the interaction used in the model have almost no effect on the finite absorption of UV laser radiation on the 100-ns interval of integration of the equations under consideration. An exact knowledge of these constants will be important for modelling relaxation processes on longer time intervals and in the case of the second model, which is described below.

Emission of XeF, KrF, and ArF lasers with photon energies of 3.5, 5.0, and 6.3 eV falls into different regions of the absorption band of F centres in MgF_2 , and therefore the model was debugged by comparing its predictions with the experimental results [3, 6, 9, 10, 15, 16].

The experimental results of primary importance were the conservation of the form of excimer laser pulses after their transmission through MgF_2 samples at the moment of their irradiation with an electron beam and the absorption recorded under these conditions [9, 10, 16]. The conservation of the form of probe laser pulse indicated to two important facts, which are taken into account in the structure of equations.

(1) The relaxation time of the major absorbing components does not exceed several nanoseconds. This means that quasi-stationary absorption induced by an electron beam in the F center band in a MgF_2 crystal is caused mainly by self-trapped excitons.

(2) The efficiency of production of long-lived F and H -centres is not greater than 5% of the total number of self-trapped excitons. Otherwise, a noticeable increase in absorption would be observed by the end of a 80-ns pulse of ionising radiation.

When debugging the system of kinetic equations by comparing its solutions with the experiments on absorption induced by an electron beam, we took into account the experimental distribution of specific absorbed irradiation dose along the sample $D(x)$ [9, 10], which specified the ionisation rate in the form $W_1(x) = D(x)/3TE_g$, where x is the coordinate along a sample; T is the pulse duration; and E_g is the band gap of a crystal ($3E_g$ is the average energy of electron-hole pair production). Because the laser radiation intensity in these experiments was $\sim 1 \text{ MW cm}^{-2}$, the product βJ^2 was almost equal to zero, and electronic excitations in a crystal were produced by an electron beam.

The optical density Δ was calculated by integrating induced absorption obtained from equations ($K_{\Sigma} = \sigma_4 S^* + \sigma_5 S_1 + \sigma_6 S_3 + \sigma_8 F^* + \sigma_9 F + \sigma_{10} \alpha + \beta J$) over the sample thickness, and the result was compared with the experimental value. Here, absorption is mainly determined by S_1 , S_3 , and F centres. The cross section for laser radiation absorption by these complexes ($\sigma_5 = \sigma_6 = \sigma_9$) was used in simulation of experimental data. The quantities τ_{56} and τ_{67} and also $X_{45} = X_{46}$ and X_{47} , which determine the concentrations of the corre-

sponding short and long-lived absorbing components, were found to be rigidly related to these cross sections. The agreement of calculated and experimental data on absorption induced by ionising radiation, the form of a probing laser pulse transmitted through a sample (Fig. 1), and residual absorption was obtained within the limits of 20% of the nominal values chosen for the above parameters of the model.

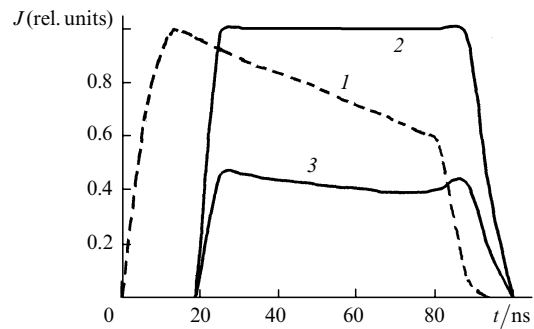


Figure 1. Pulses of an electron beam (1), KrF laser radiation incident on a MgF_2 sample (2), and transmitted laser radiation (3).

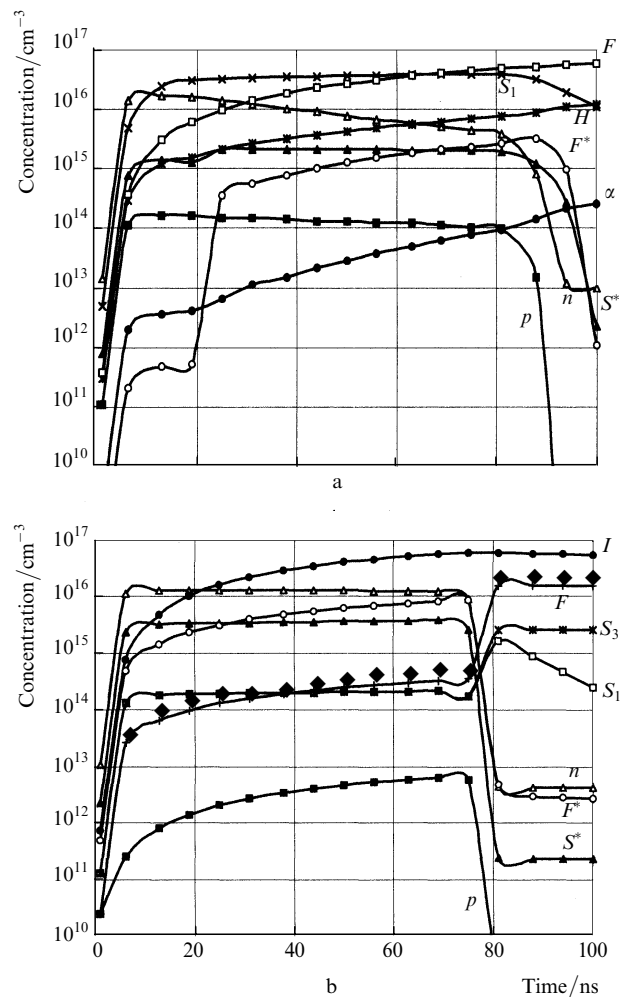


Figure 2. Time behaviour of component concentrations in a MgF_2 sample exposed to an electron beam with a specific power of 100 MW cm^{-3} (a) and to laser radiation with an intensity of 1 GW cm^{-2} (b). Shapes of laser and electron beam pulses are shown in Fig. 1.

Табл.1.

Components	Version 1		Version 2		Version 3	
	Concentration/cm ⁻³	Absorption coefficient/cm ⁻¹	Concentration/cm ⁻³	Absorption coefficient/cm ⁻¹	Concentration/cm ⁻³	Absorption coefficient/cm ⁻¹
Electrons	5.9×10^{15}	–	5.3×10^{15}	–	1.3×10^{16}	–
Holes	1.3×10^{14}	–	6.3×10^{11}	–	4.7×10^{12}	–
V_k	4.3×10^{16}	–	4.5×10^{15}	–	1.5×10^{16}	–
S^*	2.3×10^{15}	4.6×10^{-3}	9.1×10^{14}	1.8×10^{-3}	3.6×10^{15}	7.2×10^{-3}
S_1	4.3×10^{16}	2.94	9.8×10^{13}	6.8×10^{-3}	2.1×10^{14}	1.5×10^{-2}
S_3	4.8×10^{16}	3.29	9.9×10^{13}	7.0×10^{-3}	2.1×10^{14}	1.5×10^{-2}
H	6.2×10^{15}	–	2.5×10^{15}	–	4.2×10^{15}	–
F^*	2.1×10^{15}	4.0×10^{-3}	1.5×10^{15}	3.0×10^{-3}	6.2×10^{15}	1.2×10^{-2}
F	4.1×10^{16}	2.8	9.6×10^{13}	6.7×10^{-3}	2.5×10^{14}	1.8×10^{-2}
α	5.5×10^{13}	5.4×10^{-7}	10^{16}	10^{-4}	3.7×10^{16}	3.7×10^{-4}
I	3.7×10^{16}	–	9.2×10^{15}	–	4.0×10^{16}	–
$K_{\Sigma}/\text{cm}^{-1}$	9.1	–	$2.7 \cdot 10^{-2}$	–	$7.0 \cdot 10^{-2}$	–
$\beta J/\text{cm}^{-1}$	–	–	$1.5 \cdot 10^{-3}$	–	$3 \cdot 10^{-4}$	–

The coefficients entering into the above equations had the following values: $K_{13} = 5 \times 10^{-8} \text{ cm}^3 \text{ s}^{-1}$, $K_{17} = 2 \times 10^{-8} \text{ cm}^3 \text{ s}^{-1}$, $K_{110} = 3 \times 10^{-8} \text{ cm}^3 \text{ s}^{-1}$, $K_4 = 10^{-7} \text{ cm}^3 \text{ s}^{-1}$, $K_5 = 10^{-8} \text{ cm}^3 \text{ s}^{-1}$, $K_{56} = K_{65} = 5 \times 10^{-8} \text{ cm}^3 \text{ s}^{-1}$, $K_6 = 10^{-8} \text{ cm}^3 \text{ s}^{-1}$, $K_{78} = 10^{-10} \text{ cm}^3 \text{ s}^{-1}$, $K_{79} = 10^{-11} \text{ cm}^3 \text{ s}^{-1}$, $K_8 = 10^{-7} \text{ cm}^3 \text{ s}^{-1}$, $K_{811} = 10^{-10} \text{ cm}^3 \text{ s}^{-1}$, $K_{911} = 10^{-11} \text{ cm}^3 \text{ s}^{-1}$, $K_{1011} = 10^{-10} \text{ cm}^3 \text{ s}^{-1}$; $\tau_2 = 10^{-11} \text{ s}$, $\tau_3 = 10^{-5} \text{ s}$, $\tau_4 = 10^{-10} \text{ s}$, $\tau_5 = 10^{-8} \text{ s}$, $\tau_{57} = 6 \times 10^{-7} \text{ s}$, $\tau_6 = 10^{-4} \text{ s}$, $\tau_{67} = 6 \times 10^{-7} \text{ s}$, $\tau_8 = 5 \times 10^{-10} \text{ s}$; $\sigma_4 = 2 \times 10^{-18} \text{ cm}^2$, $\sigma_5 = \sigma_6 = \sigma_7 = 7 \times 10^{-17} \text{ cm}^2$, $\sigma_8 = 2 \times 10^{-18} \text{ cm}^2$, $\sigma_{10} = 10^{-20} \text{ cm}^2$ (the values of σ_i correspond to $\lambda = 248 \text{ nm}$); $X_{45} = X_{46} = 0.45$, $X_{47} = 0.03$. The time behaviour of concentrations of the complexes taken into account in the model for two regimes of irradiation of MgF_2 samples by an electron beam and laser radiation is shown in Fig. 2.

The model with the coefficients presented above was tested by comparing its predictions with the experimental results on nonlinear absorption of KrF laser radiation in MgF_2 [15]. In these experiments, the intensity of the 80-ns laser pulse was $\sim 0.1 - 0.5 \text{ GW cm}^{-2}$, and nonlinear absorption was measured to be 0.05 cm GW^{-1} . For this case, we set in the model $W_1 = 0$, and β was taken equal to 0.003 cm GW^{-1} . This value of β was obtained by using picosecond pulses [17].

The absorption of two photons with a total energy of 10 eV by a MgF_2 crystal can induce the electronic transition from the valence band to one of the high exciton levels. In our equations, this corresponds to the S^* state. When modelling the above experiments, we refined the values presented above for σ_4 , σ_8 , and σ_{10} . The resulting nonlinear absorption predicted by the model for this case agrees with the experimental data for $J < 0.6 \text{ GW cm}^{-2}$ (Fig. 3). For higher laser radiation intensities, the calculated absorption increases by a factor of about two.

In this case, the reason responsible for an increase in nonlinear absorption in experiments with nanosecond pulses (see the table) becomes also clear. In the case of a long pulse, self-trapped excitons and F centres formed upon two-photon absorption of laser radiation have time to convert several additional quanta, which accounts for an increase in nonlinear absorption in this regime. In this case, pulses whose duration exceeds the formation time for the major absorbing centres (here, they represent STEs), which is not greater than 10^{-10} s [6, 8, 11, 12], may be treated as long.

The concentrations in a MgF_2 crystal calculated for the components taken into account in the model and the contribution of these components to absorption of laser radiation at the wavelength 248 nm by the middle of a 80-ns irradiation pulse are presented in the table.

For version 1, we present results obtained upon irradiation of MgF_2 by an electron beam with a specific power of 100 MW cm^{-3} . This specific power was reached in the near-surface region of a crystal irradiated by an electron beam with the energy density of 0.5 J cm^{-3} [16]. The intensity of probing laser radiation was 1 MW cm^{-2} .

For versions 2 and 3, we present the concentrations of components in experiments where MgF_2 was exposed only to laser radiation with intensity of 0.5 and 1.0 GW cm^{-2} , respectively. One can see from the last two rows of the table an extent to which absorption by intermediate complexes in these two versions exceeds two-photon absorption. The time behaviour of component concentrations for the first and third versions is shown in Fig. 2.

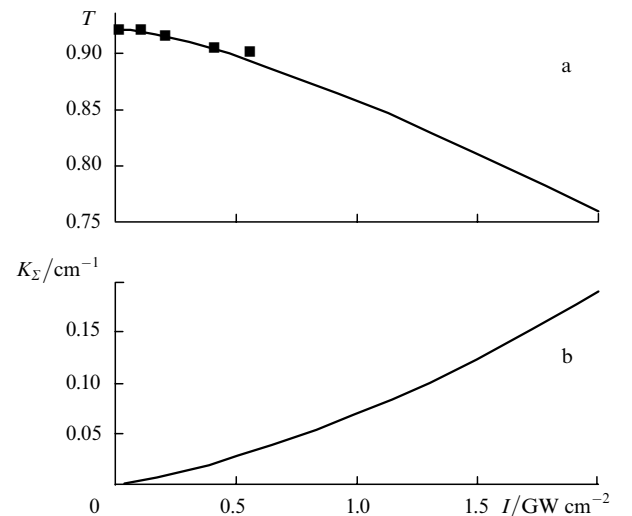


Figure 3. Calculated (curve) and experimental [15] (points) dependences of the transmission T of a MgF_2 crystal 1 cm thick on the KrF laser intensity (a) and the calculated dependence of absorption K_{Σ} in MgF_2 at $\lambda = 248 \text{ nm}$ on the laser radiation intensity (b).

For simplification, the dependences $S_3(t)$, $I(t)$, and $V_k(t)$ are not presented in Fig. 2a because $S_3(t)$ coincides with $S_1(t)$, $I(t)$ coincides with $F(t)$, and the dependence $V_k(t)$ is simple, namely, the concentration monotonically increases from approximately $2 \times 10^{16} \text{ cm}^{-3}$ at the beginning of a pulse to $4.5 \times 10^{16} \text{ cm}^{-3}$ at the end. Fig. 2b presents no dependences $V_k(t)$, $H(t)$, and $\alpha(t)$. For V_k and H centres, concentrations in the 10 – 100-ns range are almost constant and approximately equal to 1.5×10^{16} and $4.2 \times 10^{15} \text{ cm}^{-3}$, respectively, and the dependence $\alpha(t)$ coincides with $I(t)$.

Using the model analysed here one can also qualitatively describe the experimental data on the ray strength of MgF_2 at $\lambda = 248 \text{ nm}$ for 80-ns pulses [15]. The calculation shows that a crystal exposed to breakdown laser radiation intensities taken from the experiment is heated up to the melting temperature, and this is a criterion of the onset of laser damage of optical materials [18]. Note that in this case the coefficients entering into the system of basis equations are assumed to be constant throughout the range of temperature variation from 300 to 1600 K. It is obvious that this assumption should be verified in detail before using the model for the quantitative description of crystals under study in extreme conditions of their exposure to high-intensity laser radiation.

In conclusion of the section we note the following result predicted by the model. The saturation intensity for absorption induced by laser radiation in MgF_2 in the quasi-stationary regime at $\lambda = 248 \text{ nm}$ is $\sim 10 \text{ MW cm}^{-2}$. An experimental test of this statement will be decisive for the verification of the validity of the model.

3. Absorption of laser radiation by F_2^- complexes

When moving into the UV region, one can observe in the absorption spectrum of crystals wide absorption bands of V_k and H centres behind the absorption band of F centres. These new defects represent an F_2^- -molecule localised in one or two anionic sites of a lattice and insignificantly differ only in the internuclear distance [6–8, 11, 12]. Their strongest absorption bands in the UV region virtually merge together [11, 12]. The capture of a quantum in the region of the fundamental absorption band of these centres causes a decomposition of the F_2^- molecule into the F^- ion and a free hole [8, p. 73], which rapidly localises.

This process can be described using the slightly modified above system of equations. One should bear in mind that absorption by all centres taken into account in the first model will have a considerably smaller cross section. Here, the final electron state (the conduction band) is changed as well. Moreover, absorption by V_k and H centres and by the hole component of STEs is added to the model. After absorbing a photon, centres are reconstructed for $\sim 100 \text{ ps}$, and the process repeats.

As the laser radiation wavelength is decreased, the kinetics of electronic relaxation in crystals retains the specific features mentioned above until the laser photon energy becomes sufficient to transfer a binding electron of V_k or H centres to excitonic levels or the conduction band. In the latter case, the photon energy close to E_g is required. The threshold energy required for the transition to excitonic level is lower and approximately equal to the difference between the band gap and the Rydberg energy for the corresponding crystal. For MgF_2 and CaF_2 , the threshold energy of such transitions is 5 – 6 eV, and the value for BaF_2 is close to 7 eV. We

did not manage to find exact data on these transitions, but they are mentioned in the literature (see [8], p. 113). Impurity levels can also take an active part in this process.

The F_2^- ‘molecule’ formed in a crystal from an F_2^- molecule after the electronic transition to an excitonic or impurity level with a relatively long lifetime is unstable. In a time of $\sim 10^{-12} \text{ s}$, the ‘holes’ incorporated into this molecule fly apart, lose their energy, and are localised by producing new V_k and H centres or STEs. In this process, the absorption of one high-energy photon results in the production of two new absorbing centres.

In this case, the basis system of kinetic equations includes the terms taking into account centre phototransformations. As a result, it takes the form

1.
$$\frac{dn}{dt} = W_1 + \beta J^2 + (K_{811} F^* + K_{911} F) I + (\sigma_{41} S^* + \sigma_{51} S_1 + \sigma_{61} S_3 + \sigma_8 H + \sigma_9 F) J - (K_{13} V_k + K_{17} H + K_{110} \alpha) n,$$
2.
$$\frac{dp}{dt} = W_1 + \beta J^2 + (\sigma_3 V_k + \sigma_{10} \alpha) J - \frac{p}{\tau_2},$$
3.
$$\frac{dV_k}{dt} = \frac{p}{\tau_2} + (\sigma_{41} S^* + \sigma_{51} S_1 + \sigma_{61} S_3) J - \left(\frac{1}{\tau_3} + K_{13} n + \sigma_3 J \right) V_k,$$
4.
$$\frac{dS^*}{dt} = X_{34} K_{13} n V_k + (\sigma_3 V_k + \sigma_{52} S_1 + \sigma_{62} S_3 + \sigma_7 H) J - \left[\frac{1}{\tau_4} + K_4 n + (\sigma_{41} + \sigma_{42}) J \right] S^*,$$
5.
$$\frac{dS_1}{dt} = X_{45} \left(\frac{1}{\tau_4} + K_4 n \right) S^* + X_{55} \sigma_{42} S^* J - \left(\frac{1}{\tau_{50}} + \frac{1}{\tau_{57}} + K_5 n + \sigma_{51} J + \sigma_{52} J \right) S_1 - K_{56} (S_1 - S_3) n,$$
6.
$$\frac{dS_3}{dt} = X_{46} \left(\frac{1}{\tau_4} + K_4 n \right) S^* + X_{55} \sigma_{42} S^* J - \left(\frac{1}{\tau_{60}} + \frac{1}{\tau_{68}} + K_6 n + \sigma_{61} J + \sigma_{62} J \right) S_3 - K_{65} (S_3 - S_1) n,$$
7.
$$\frac{dH}{dt} = \frac{V_k}{\tau_3} + \frac{X_{47} S^*}{\tau_4} + \frac{S_1}{\tau_{57}} + \frac{S_3}{\tau_{67}} + \frac{H^*}{\tau_{12}} + (\sigma_{42} S^* + \sigma_{52} S_1 + \sigma_{62} S_3) J - (K_{17} n + K_{78} F^* + K_{79} F + \sigma_7 J) H,$$
8.
$$\frac{dF^*}{dt} = K_{110} \alpha n + (\sigma_{42} S^* + \sigma_{10} \alpha) J - \left(\frac{1}{\tau_8} + K_{89} n + K_{78} H + K_{811} I + \sigma_8 J \right) F^*,$$
9.
$$\frac{dF}{dt} = \frac{X_{47} S^*}{\tau_4} + \frac{S_1}{\tau_{57}} + \frac{S_3}{\tau_{67}} + \left(\frac{1}{\tau_8} + K_{89} n \right) F^* + (\sigma_{52} S_1 + \sigma_{62} S_3) J - (K_{79} H + K_{911} I + \sigma_9 J) F,$$

$$10. \frac{d\alpha}{dt} = \frac{V_k}{\tau_3} + (\sigma_8 F^* + \sigma_9 F)J - (K_{110}n + K_{810}H + K_{1011}I + \sigma_{10}J)\alpha,$$

$$11. \frac{dI}{dt} = K_{17}nH - (K_{811}F^* + K_{911}F + K_{1011}\alpha)I,$$

$$12. \frac{dH^*}{dt} = \sigma_7 HJ - \frac{H^*}{\tau_{12}}.$$

This system of equations represents the previous system with an additional equation for H^* , for the F atom with a large kinetic energy, which is located in one of the lattice interstices. Moreover, it includes many new phototransitions with absorption cross sections σ_{m1} and σ_{m2} ($m = 4, 5, 6$), which describe absorption by electron and hole components of the corresponding STEs. Relaxation processes are described by the same terms as in the first model. In this case, additional equations appearing from the condition of conservation of charge and number of atoms take the form

$$n + F^* + F = p + V_k + H + H^*,$$

$$H + I + H^* = F^* + F + \alpha.$$

The total absorption in this version is determined in the following way:

$$\begin{aligned} K_\Sigma &= (\sigma_3 V_k + \sigma_{42} S^* + \sigma_{52} S_1 + \sigma_{62} S_3 + \sigma_7 H) \\ &+ (\sigma_{41} S^* + \sigma_{51} S_1 + \sigma_{61} S_3 + \sigma_8 F^* + \sigma_9 F + \sigma_{10} \alpha) \\ &= \sigma_3 (V_k + S^* + S_1 + S_3 + H) + \sigma_8 (S^* + F^*) \\ &+ \sigma_9 (S_1 + S_3 + F) + \sigma_{10} \alpha + \beta J. \end{aligned}$$

These relations follow from the fact that absorption by V_k and H centres and by the hole component of STEs has approximately the same cross sections ($\sigma_3 = \sigma_{42} = \sigma_{52} = \sigma_{62} = \sigma_7$), as well as absorption by highly excited complexes ($\sigma_8 = \sigma_{41}$) and F centres of various nature ($\sigma_{51} = \sigma_{61} = \sigma_9$).

This model was verified using the experimental data for CaF_2 [15, 16, 19]. Calculations show that here, at laser radiation intensities above 0.1 GW cm^{-2} , multiple absorption of photons by each colour centre during long pulses provides a considerably higher energy release in comparison with direct two-photon absorption.

To demonstrate substantial difference in the behaviour of crystals under the action of laser radiation in the first and second models, consider equations for the total concentration N of quasi-particles in a lattice. For this purpose we sum equations of the corresponding systems, from the second equation to the last one, and find

$$\begin{aligned} \frac{dN}{dt} &= \beta J^2 - \left[\frac{S_1}{\tau_5} + \frac{S_3}{\tau_6} + 2(K_{78}F^* + K_{79}F)H \right. \\ &\quad \left. + 2(K_{811}F^* + K_{911}F)I + 2K_{1011}I\alpha \right] \\ &= \beta J^2 - R \approx \beta J^2 - \mu N^2, \end{aligned} \quad (1)$$

$$\begin{aligned} \frac{dN}{dt} &= \beta J^2 + (\sigma_3 V_k + 2\sigma_{42} S^* + 2\sigma_{52} S_1 \\ &\quad + 2\sigma_{62} S_3 + \sigma_7 H)J - R \approx \beta J^2 + \sigma_{e2} NJ - \mu N^2. \end{aligned} \quad (2)$$

The last expressions in (1) and (2) were obtained in the following way. The component concentrations were represented in the form $\varkappa_i N$, where \varkappa_i is the fraction of the given component in N . After that N and N^2 were factored out, and the terms remaining in brackets were denoted by μ and σ_{e2} , which gave the resulting relations.

One can see from (1) that the first model gives in the quasi-stationary regime the concentration $N = (\beta/\mu)^{1/2} J$. In this regime, the expression for the absorption coefficient K_Σ takes the form

$$\begin{aligned} K_\Sigma &= \beta J + \sigma_{e1} N = \left[\beta + \sigma_{e1} \left(\frac{\beta}{\mu} \right)^{1/2} \right] J \\ &= \left[1 + \sigma_{e1} \left(\frac{1}{\beta\mu} \right)^{1/2} \right] \beta J, \end{aligned} \quad (3)$$

where σ_{e1} is the effective cross section for absorption by all defects. It is evident that the expression in square brackets represents the coefficient showing an extent to which nonlinear absorption for long pulses is higher than the corresponding two-photon absorption for short pulses. One can see from (1) and (3) that quasi-particles in the first model are produced only through two-photon absorption (or due to another ioniser).

In the second model, quasi-particles are additionally produced through one-photon absorption of laser radiation by V_k and H centres and by the hole component of STEs. If the production of absorbing complexes is dominated by the linear mechanism, which is realised in the presence of impurity defects with concentration of 10^{15} cm^{-3} and above, we find from (2) that the concentration in the quasi-stationary regime is $N = (\sigma_{e2}/\mu)J$. In this case, the expression for the effective nonlinear absorption takes the form

$$K_\Sigma = \left(\beta + \frac{\sigma_{e2}^2}{\mu} \right) J = \left(1 + \frac{\sigma_{e2}^2}{\mu\beta} \right) \beta J. \quad (4)$$

One can see that here nonlinear absorption for long pulses is also considerably higher than two-photon absorption for short picosecond pulses. This can explain a high nonlinear absorption measured in Ref. [19] for 80-ns laser pulses with $\lambda = 248 \text{ nm}$ in CaF_2 with impurities.

In each model, concentration reaches a stationary level under the action of a rectangular laser pulse in its own regime. In the first model, N linearly increases with time at the initial stage. In the second model, the number of particles exponentially increases, which gives evidence of the avalanche nature of the development of laser radiation absorption [20]. However, in both cases, the summary quasi-particle concentration in quasi-stationary regions linearly depends on the laser radiation intensity.

A similar increase in nonlinear absorption for long pulses was observed for semiconductors exposed to IR laser radiation [21]. In this case, additional absorption was provided by free electrons. For wide-gap crystals exposed to UV laser radiation, most notably to VUV radiation, the contribution of free electrons to absorption sharply decreases. Here, absorption is governed by other quasi-particles, with natural

frequencies of electronic transitions close to the laser radiation frequency.

From equations (1)–(4), it follows that the two-particle recombination coefficient K_{1011} and the cross section for dissociative disintegration of V_k centres into two holes σ_3 are of critical importance in the models. According to our calculations, precisely these factors make the dominant contribution to μ and to σ_{e1} and σ_{e2} . Because of this, the determination of K_{1011} and σ_3 is of prime importance in adapting a model to a concrete crystal or a concrete laser radiation wavelength.

This is of particular importance for the second model, which is considerably more complicated than the first one and requires the analysis of a considerably larger number of details, which is beyond the scope of this paper. Because of this, concrete examples of application of the second model will be analysed elsewhere, and here we only present the conclusions obtained from analytical expressions (2) and (4).

4. Conclusions

Thus, the description of the interaction of intense UV and VUV laser pulses of duration above 1 ns with crystals of fluorides of rare-earth elements requires a consideration of the electronic states formed in crystals upon recombination of electron-hole pairs. This is caused by the fact that the energy absorbed up on transitions between these states is tens times greater than that for the classical two-photon absorption.

We analysed two versions of numerical models, which describe in the gas-kinetic approximation the behaviour of the electronic states of crystals as quasi-particles. In the first version, the laser radiation wavelength lies in the absorption region of F centres, and in the second version it lies in the region of H centre dissociation into two holes. Both models describe mechanism responsible for an increase in nonlinear absorption of laser radiation in MgF_2 , CaF_2 , and BaF_2 crystals for nanosecond pulses in comparison with picosecond pulses. The models can also be used for the description of experiments with simultaneous action of ionising and laser radiation on crystal.

The models proposed in the paper are based on the modern concepts of defect formation and relaxation in the anion crystal sublattice. These processes are much alike not only in the group of MgF_2 , CaF_2 , and BaF_2 crystals considered here, but also in other ionic crystals, in particular, in alkali halide crystals. Because of this, upon the appropriate choice of coefficients in the systems of kinetic equations presented here, they can be used for the analysis of experiments on the action of ionising and laser radiation in this wide class of optical materials.

Acknowledgements. We are grateful to V S Barabanov for his help in calculations and to A G Molchanov and Ch B Lushchik for their fruitful consultations on some question studied here. This work was supported by the Russian Foundation for Basic Research (Grant No. 98-02-16562).

References

1. Fahlen T S *IEEE J. Quantum Electron.* **8** 1260 (1980)
2. Kurosawa K, Sasaki V, Okuda M, et al. *Rev. Sci. Instrum.* **61** 728 (1990)
3. Apinov A, Budina N E, Reiterov V M, Shishatskaya L P *Opt.-Mekh. Prom-st.* No. 8 10 (1983)
4. Mann K, Eva E, Granitza B *Proc. SPIE* **2714** 2 (1995)
5. Kuzuu N *Proc. SPIE* **2714** 4; 71 (1995)
6. Williams R T *Opt. Eng.* **28** 1024 (1989)
7. Jones S C, Braunlich P, et al. *Opt. Eng.* **28** 1039 (1989)
8. Lushchik Ch B, Lushchik A Ch *Raspad Elektronnykh Vozbuzhdenii s Obrazovaniem Defektov v Tverdykh Telakh (Decay of Electronic Excitations with Defect Formation in Solids)* (Moscow: Nauka, 1985) p. 101
9. Barabanov V S, Morozov N V, Sergeev P B *Kvantovaya Elektron. (Moscow)* **18** 1364 (1991) [*Sov. J. Quantum Electron.* **21** 1250 (1991)]
10. Barabanov V S, Morozov N V, Sergeev P B *J. Non-Cryst. Solids* **149** 102 (1992)
11. Stoneham A M *Theory of Defects in Solids: the Electronic Structure of Defects in Insulators and Semiconductors* (Oxford: Clarendon Press, 1975)
12. Aluker E D et al. *Elektronnye Vozbuzhdeniya i Radiolyuminesentsiya Shchelochno-Galoidnykh Kristallov (Electronic Excitations and Radioluminescence of Alkali Halide Crystals)* (Riga: Zinatne, 1979) p. 40
13. Aluker E D, Gavrilov V V, et al. *Fiz. Tverd. Tela (Leningrad)* **26** 321 (1984)
14. Sergeev P B *Kratkie Soobshch. Fiz. FIAN* No. 5 39 (1999)
15. Barabanov V S, Morozov N V, Sagitov S I, Sergeev P B *J. Sov. Laser Res.* **14** 294 (1993)
16. Barabanov V S, Sergeev P B *Kvantovaya Elektron. (Moscow)* **22** 745 (1995) [*Quantum Electron.* **25** 717 (1995)]
17. Taylor A J et al. *Opt. Lett.* **13** 814 (1988)
18. Manenkov A A, Prokhorov A M *Usp. Fiz. Nauk* **148** 179 (1986)
19. Morozov N V, Reiterov V M, Sergeev P B *Kvantovaya Elektron. (Moscow)* **29** 141 (1999) [*Quantum Electron.* **29** 979 (1999)]
20. Semenov N N *Tsepnye Reaktsii (Chain Reactions)* (Moscow: Nauka, 1986) p. 68
21. Gibson A F, Hatch C B, Maggs P N D, et al. *J. Phys. C* **9** 3259 (1976)